THE JOURNAL OF BIOLOGICAL CHEMISTRY
Vol. 277, No. 42, Issue of October 18, pp. 39777–39785, 2002

Printed in U.S.A.

Paclitaxel-resistant Human Ovarian Cancer Cells Undergo c-Jun NH_2-terminal Kinase-mediated Apoptosis in Response to Noscapine*

Received for publication, April 23, 2002, and in revised form, August 7, 2002
Published, JBC Papers in Press, August 14, 2002, DOI 10.1074/jbc.M203927200

Jun Zhou‡§, Kamlesh Gupta¶, Joyce Yao‡§, Keqiang Ye‖, Dulal Panda¶, Paraskevi Giannakakou, and Harish C. Joshi§‡‡**

*From the ‡Graduate Program in Biochemistry, Cell and Developmental Biology, §Department of Cell Biology, ‖Department of Pathology, the **Winship Cancer Institute, Emory University School of Medicine, Atlanta, Georgia 30322, and the ¶Bhupat and Jyoti Mehta School of Biosciences and Bioengineering, Indian Institute of Technology, Bombay, Mumbai 400076, India*

We have previously discovered the opium alkaloid noscapine as a microtubule interacting agent that binds to tubulin, alters the dynamics of microtubule assembly, and arrests mammalian cells at mitosis (Ye, K., Ke, Y., Keshava, N., Shanks, J., Kapp, J. A., Tekmal, R. R., Petros, J., and Joshi, H. C. (1998) *Proc. Natl. Acad. Sci. U. S. A.* 95, 1601–1606; Ye, K., Zhou, J., Landen, J. W., Bradbury, E. M., and Joshi, H. C. (2001) *J. Biol. Chem.* 276, 46697–46700; Zhou, J., Panda, D., Landen, J. W., Wilson, L., and Joshi, H. C. (2002) *J. Biol. Chem.* 277, 17200–17208). Here we show that noscapine does not compete with paclitaxel for tubulin binding and can efficiently inhibit the proliferation of both paclitaxel-sensitive and paclitaxel-resistant human ovarian carcinoma cells (*i.e.* the parental cell line 1A9 and two derivative cell lines, 1A9PTX10 and 1A9PTX22, which harbor β-tubulin mutations that impair paclitaxel-tubulin interaction (Giannakakou, P., Sackett, D. L., Kang, Y. K., Zhan, Z., Buters, J. T., Fojo, T., and Poruchynsky, M. S. (1997) *J. Biol. Chem.* 272, 17118–17125). Strikingly, these cells undergo apoptotic death upon noscapine treatment, accompanied by activation of the c-Jun NH_2-terminal kinases (JNK). Furthermore, inhibition of JNK activity by treatment with antisense oligonucleotide or transfection with dominant-negative JNK blocks noscapine-induced apoptosis. These findings thus indicate a great potential for noscapine in the treatment of paclitaxel-resistant human cancers. In addition, our results suggest that the JNK pathway plays an essential role in microtubule inhibitor-induced apoptosis.

Microtubules are cytoskeletal components that play a critical role in many cellular processes, such as maintenance of cell shape and polarity, intracellular transport of vesicles and organelles, and beating of cilia and flagella. During cell division, microtubules form a bipolar microtubule array, called the mitotic spindle, that functions in the distribution of chromosomes into two daughter cells (1). Assembled from αβ-tubulin heterodimers, microtubules are highly dynamic structures that alternate between periods of growth and shortening (2), and the dynamic instability property is crucial for microtubules to carry out many of their cellular functions (3). Disruption of microtubule dynamics can lead to the formation of abnormally stable or unstable microtubules, thereby preventing the normal dynamic rearrangements of the microtubule network required for cell proliferation (4).

One group of agents that target microtubules, such as colchicine, nocodazole, and the vinca alkaloids, inhibit microtubule polymerization. Another group of agents, such as taxoids and epothilones, however, promote microtubule polymerization and stabilize microtubules. Nevertheless, they all disrupt microtubule dynamics, block cell cycle progression at mitosis, and then cause cell death (4). This provides the molecular basis for the use of microtubule targeting compounds in chemotherapeutic treatment of human cancers.

Microtubule drugs currently in clinical use for cancer chemotherapy include paclitaxel (Fig. 1*A*), docetaxel, and the vinca alkaloids. Specifically, paclitaxel has proven effective against refractory ovarian cancer, metastatic breast cancer, and non-small cell lung cancer (5, 6), and the vinca alkaloids are effective against cancer types such as lymphoma, leukemia, and Kaposi's sarcoma (7, 8). Unfortunately, the toxicity and low aqueous solubility have limited the applicability of taxoids and vinca alkaloids in cancer chemotherapy. Moreover, their use has been hampered by the development of drug resistance contributed by multifactorial mechanisms, such as overexpression of P-glycoprotein (9, 10), altered expression of tubulin isotypes (11), and the presence of tubulin mutations (12). Therefore, development and/or discovery of microtubule-based compounds are in demand, especially for the treatment of human cancers resistant to currently used drugs.

We have previously identified noscapine (Fig. 1*A*), an opium alkaloid, as a microtubule targeting agent that binds stoichiometrically to tubulin and alters tubulin conformation (13). Like many other microtubule drugs, noscapine suppresses microtubule dynamics, arrests mammalian cells at mitosis, causes apoptosis, and exhibits potent antitumor activity (13–15). However, distinct from other microtubule drugs, noscapine does not affect the total polymer mass of tubulin and does not cause gross deformation of cellular microtubules even at high concentrations (15). In addition, the low toxicity, water solubility, and feasibility for oral administration are very valuable advantages of noscapine over many other microtubule drugs for future clinical use in cancer chemotherapy (16–19).

In this study, we find that noscapine does not compete with paclitaxel for tubulin binding and can efficiently inhibit the proliferation of both paclitaxel-sensitive and paclitaxel-resistant human ovarian carcinoma cells. In addition, noscapine causes these cells to die through the c-Jun NH_2-terminal ki-

* This work was supported by a grant from the National Institutes of Health (to H. C. J.) and an award from the Association for the Cure of Cancer of the Prostate (CaP CURE) (to D. P.). The costs of publication of this article were defrayed in part by the payment of page charges. This article must therefore be hereby marked "*advertisement*" in accordance with 18 U.S.C. Section 1734 solely to indicate this fact.

‡‡ To whom correspondence should be addressed: Dept. of Cell Biology, Emory University School of Medicine, 615 Michael St., Atlanta, GA 30322. Tel.: 404-727-0445; Fax: 404-727-6256; E-mail: joshi@cellbio.emory.edu.

nase (JNK)[1]-mediated apoptosis pathway. These findings thus not only offer a rationale for the use of noscapine in the treatment of paclitaxel-resistant human cancers, but they also provide important insights into the molecular mechanisms by which microtubule targeting agents inhibit cell proliferation and cause cell death.

EXPERIMENTAL PROCEDURES

Materials—Goat brain microtubule proteins were isolated in the presence of 1 M glutamate by two cycles of polymerization and depolymerization (20). Tubulin was purified from the microtubule proteins by phosphocellulose chromatography as described previously (21). The tubulin solution was stored at −80 °C until future use. Protein concentration was determined by the method of Bradford using bovine serum albumin (BSA) as a standard (22). The dominant-negative JNK1 expressing plasmid with a FLAG tag insertion, pCDNA3(FLAG)-JNK-dn, and the pCDNA3 vector with a FLAG tag insertion, pCDNA3(FLAG), were kindly provided by Dr. R. J. Davis (University of Massachusetts, Worcester). Noscapine (97% purity) was purchased from Aldrich (Milwaukee, WI). The noscapine stock solution was prepared at 100 mM in dimethyl sulfoxide (Me_2SO) and stored at −20 °C until use. Paclitaxel was from Sigma and dissolved in Me_2SO as a 10 mM stock solution. Fluorescent paclitaxel was from Molecular Probes (Eugene, OR).

Cell Culture—The 1A9 cell line is a clone of the human ovarian carcinoma cell line, A2780 (23). The two paclitaxel-resistant cell lines, 1A9PTX10 and 1A9PTX22, were isolated as individual clones in a single-step selection, by exposing 1A9 cells to 5 ng/ml paclitaxel in the presence of 5 μg/ml verapamil, a P-glycoprotein antagonist (12). They were all cultured in RPMI 1640 medium (Invitrogen) supplemented with 10% fetal bovine serum (Invitrogen) at 37 °C in a 5% CO_2, 95% air atmosphere as monolayers in tissue culture plates or on glass coverslips. Paclitaxel-resistant 1A9PTX10 and 1A9PTX22 cell lines were maintained in 15 ng/ml paclitaxel and 5 μg/ml verapamil continuously, but were cultured in drug-free medium for 7 days prior to each experiment.

Competitive Tubulin Binding Assay—The effect of noscapine on paclitaxel binding to tubulin was measured using fluorescent paclitaxel. In brief, microtubules were polymerized from purified goat brain tubulin in the presence of 10% Me_2SO, and preformed microtubules were incubated with different concentrations of paclitaxel (20 and 40 μM), noscapine (50 and 100 μM), or the vehicle solution Me_2SO alone as a control. Fluorescent paclitaxel was then added to each of these solutions and the fluorescence intensity was measured using a JASCO FP-6500 spectrofluorometer equipped with a constant temperature water-circulating bath (JASCO Intl. Co., Tokyo, Japan). Spectra were taken by multiple scans, and buffer blank values were subtracted from all measurements. A 0.3-cm path length cuvette was used for all fluorescence measurements to minimize the inner filter effects.

In Vitro Cell Proliferation Assay—Cytotoxicity assays were performed in 96-well plates using the sulforhodamine B assay as previously described (24). In brief, 2×10^3 cells were seeded in each well and incubated with gradient concentrations of noscapine for 72 h. The cells were then fixed with 50% trichloroacetic acid and stained with 0.4% sulforhodamine B dissolved in 1% acetic acid. The cells were then washed with 1% acetic acid to remove unbound dye. The protein-bound dye was extracted with 10 mM Tris base to determine the optical density at 564 nm wavelength using a SPECTRAmax PLUS 384 microplate spectrophotometer (Molecular Devices, Sunnyvale, CA). Each experiment was repeated three times.

Immunofluorescence Microscopy—Immunofluorescence microscopy was performed as previously described with minor modifications (15, 25, 26). To visualize microtubules, human ovarian caricinoma cells grown on glass coverslips were fixed with cold (−20 °C) methanol for 5 min and then washed with phosphate-buffered saline (PBS) for 5 min. Nonspecific sites were blocked by incubating with 100 μl of 2% BSA in PBS at 37 °C for 15 min. A mouse monoclonal antibody against α-tubulin (DM1A, Sigma) was diluted 1:500 in 2% BSA/PBS and incubated (100 μl) with the coverslips at 37 °C for 2 h. Cells were then washed with 2% BSA/PBS for 10 min at room temperature before incubating with a 1:100 dilution of a fluorescein isothiocyanate (FITC)-labeled donkey anti-mouse IgG antibody (Jackson ImmunoResearch, Inc., West Grove, PA) at 37 °C for 1 h. Coverslips were then rinsed with 2% BSA/PBS for 10 min and incubated with propidium iodide (0.5 μg/ml) for 30 s at room temperature before they were mounted with Aqua-Mount (Lerner Laboratories, Pittsburgh, PA) containing 0.01% 1,4-diazobicyclo(2,2,2)octane (DABCO, Sigma). Cells were examined with a Zeiss Axiovert 135 fluorescence microscope using a ×100/1.3 oil lens (Plan-NEOFLUAR, Carl Zeiss, Inc., Thornwood, NY). Propidium iodide staining of the nuclei was also used to measure apoptotic percentages in this study. Cells with three or more visible chromatin masses were considered apoptotic.

Changes of cellular phosphorylated c-Jun level were visualized by immunofluorescence microscopy as previously described (27). In brief, cells grown on glass coverslips were fixed with 4% paraformaldehyde in PBS for 20 min at room temperature, and then permeabilized with 0.5% IGEPAL CA-630 (Sigma) in PBS for 30 min, and blocked in 2% BSA/PBS for 20 min at room temperature. A mouse monoclonal antibody against phosphorylated c-Jun (Santa Cruz Biotechnology, Santa Cruz, CA) was diluted 1:500 in 2% BSA/PBS and incubated with the cells for 2 h at 37 °C. Cells were then washed with 2% BSA/PBS for 10 min at room temperature before incubating with a 1:100 dilution of a FITC-labeled donkey anti-mouse IgG antibody (Jackson ImmunoResearch) at 37 °C for 1 h. Coverslips were rinsed with 2% BSA/PBS for 10 min and then mounted and examined by microscopy as described above.

Terminal Deoxynucleotidyltransferase-mediated dUTP Nick-end Labeling (TUNEL) Assay—The TUNEL assay was performed by using the *in situ* cell detection kit (FITC) following the manufacturer's instructions (Roche Molecular Biochemicals). In brief, cells grown on glass coverslips were fixed by a freshly prepared paraformaldehyde solution (4% in PBS, pH 7.4) for 1 h at room temperature. Coverslips were then washed with PBS and incubated in permeabilization solution (0.1% Triton X-100, 0.1% sodium citrate) for 2 min on ice. Then, 50 μl of TUNEL reaction mixture was added on coverslips and incubated in a humidified chamber for 1 h at 37 °C in the dark. Finally, cells were mounted and examined by microscopy as described above. TUNEL-positive (apoptotic) cells stained bright green (see Fig. 4*A*). Comparisons in apoptotic cell ratio between the 1A9 cell line and the two mutant cell lines were analyzed by the Student's *t* test. Statistical difference was considered significant if *p* values were less than 0.05.

Annexin V Staining Assay—The annexin V staining assay was performed by using the annexin V apoptosis detection kit (FITC) following the manufacturer's protocol (Pharmingen). Briefly, cells were washed with PBS and then resuspended in 100 μl of binding buffer (10 mM HEPES, pH 7.4, 140 mM NaCl, 2.5 mM $CaCl_2$). Cells were incubated with 5 μl of FITC-conjugated annexin V for 15 min at room temperature in the dark. Then 400 μl of binding buffer was added, and cells were analyzed by flow cytometry using a Coulter Elite flow cytometer (Beckman Coulter, Inc., Fullerton, CA). The M1 and M2 gates demarcate annexin V-FITC negative and positive staining populations, respectively (see Fig. 4*B*). Comparisons in apoptotic cell ratio between the 1A9 cell line and the two mutant cell lines were analyzed by the Student's *t* test as described above.

Preparation of Nuclear Extracts—Nuclear extracts were prepared by the method of Stone and Chambers (28). Briefly, cells grown in plates were collected by gentle scraping and centrifugation (1,500 × *g*, 10 min). After being washed with cold PBS, cells were suspended in 3 ml of buffer A (10 mM HEPES, pH 7.9, 1.5 mM $MgCl_2$, 10 mM KCl, 0.5 mM dithiothreitol, 20 mM β-glycerophosphate, 1 mM Na_3VO_4, 20 μg/ml aprotinin, 50 μg/ml leupeptin, 10 μM pepstatin, 0.1 μM okadaic acid, 1 mM phenylmethylsulfonyl fluoride) and then homogenized by a Dounce grinder (Fisher) followed by centrifugation at 1000 × *g* for 10 min to collect the nuclei pellet. The nuclei were then suspended in buffer A again, rehomogenized, and pelleted. Subsequently, the nuclei were lysed in buffer B (20 mM HEPES, pH 7.9, 25% glycerol, 0.6 M NaCl, 1.5 mM $MgCl_2$, 0.2 mM EDTA) for 1 h followed by centrifugation at 12,500 × *g* for 15 min. The supernatant was collected and dialyzed against 1 liter of buffer C (20 mM HEPES, pH 7.9, 20% glycerol, 0.1 M KCl, 0.2 mM EDTA, 1 mM phenylmethylsulfonyl fluoride, 0.5 mM dithiothreitol) and extracts were stored at −70 °C.

Immunoprecipitation—Polyclonal antibodies against JNK1 and protein A-agarose beads were purchased from Santa Cruz Biotechnology. Whole cell lysates were prepared with the lysis buffer (20 mM Tris, pH 7.4, 200 mM NaCl, 0.1% Nonidet P-40, 1 mM phenylmethylsulfonyl fluoride, 1 mM Na_3VO_4, 10 mM NaF), and total protein concentration was then determined in each fraction by BCA reagents (Pierce). 100 μg of total protein was immunoprecipitated with JNK1 antibody in excess and protein A-agarose beads at 4 °C overnight. The JNK precipitates were washed three times with the lysis buffer and then used either for JNK activity assay or resuspended in Laemmli's loading buffer (50 mM

[1] The abbreviations used are: JNK, c-Jun NH_2-terminal kinases; Me_2SO, dimethyl sulfoxide; PBS, phosphate-buffered saline; BSA, bovine serum albumin; FITC, fluorescein isothiocyanate; TUNEL, terminal deoxynucleotidyltransferase-mediated dUTP nick-end labeling.

Tris, pH 6.8, 100 mM dithiothreitol, 2% SDS, 0.1% bromphenol blue, 10% glycerol) for Western blot analysis of JNK protein level (see below). To examine the specificity of the immunoprecipitation procedure, protein A-agarose beads alone and protein A-agarose beads plus polyclonal antibodies against hemagglutinin (Sigma), an unrelated antibody, were used as controls.

JNK Activity Assay—The kinase assay of JNK1 was performed according to Wang *et al*. (29) with minor modifications. In brief, whole cell lysates were prepared and JNK1 was immunoprecipitated as described above. The precipitates were washed three times with the cell lysis buffer and then twice with kinase buffer (25 mM HEPES, pH 7.5, 25 mM $MgCl_2$, 25 mM β-glycerophosphate). The kinase reactions were performed by incubating the immunoprecipitates with 0.2 μg of glutathione *S*-transferase-c-Jun (Santa Cruz Biotechnology) in the reaction mixture (1 mM dithiothreitol, 0.1 mM Na_3VO_4, 10 μM ATP) at room temperature for 30 min. Laemmli's loading buffer was added to stop the reaction, and the level of c-Jun phosphorylation was revealed by Western blot analysis using monoclonal antibodies against phosphorylated c-Jun (Santa Cruz Biotechnology). The level of phosphorylated c-Jun was determined by densitometry as a measure of JNK activity, using a Lynx video densitometer (Biological Vision Inc., San Mateo, CA). Each experiment was repeated three times with duplicate densitometric determinations.

To measure the linearity of the JNK activity assay over a range of enzyme concentrations, 30, 53, 93, 163, 286, and 500 microunits of pure active JNK (Upstate Biotechnology, Lake Placid, NY) instead of JNK immunoprecipitate was used. 1 Unit of JNK is equal to 1 nM phosphate incorporated into glutathione *S*-transferase-c-Jun per min. To measure the linearity of the JNK activity assay over a range of incubation time, 286 microunits of pure active JNK instead of JNK immunoprecipitate was used, and the incubation time varied from 0 to 50 min instead of a constant time of 30 min.

Western Blot Analysis—Proteins were resolved by SDS-polyacrylamide gel electrophoresis, and the protein bands were electrophoretically transferred onto polyvinylidene difluoride membranes (Millipore, Bedford, MA). The membranes were first incubated with mouse monoclonal or rabbit polyclonal primary antibodies and then incubated with horseradish peroxidase-labeled anti-mouse or anti-rabbit secondary antibodies. Specific proteins were visualized using enhanced chemiluminescence following manufacturer's instructions (Amersham Biosciences).

Antisense Oligonucleotide Treatment—The antisense oligonucleotide experiment for inhibition of JNK1 expression was performed as previously described (30, 31). The antisense (5′-GTCACGCTTGCTTCTGCTCATGAT-3′) and sense (5′-ATCATGAGCAGAAGCAAGCGTGAC-3′) oligonucleotides specific for JNK1 were designed as reported by Seimiya *et al.* (30). These sequences represent the amino acid codons −1 to +7 of JNK1. They were synthesized with phosphorothioate substitutions and purified by high performance liquid chromatography (Integrated DNA Technologies, Coralville, IA). The oligonucleotides were dissolved in sterilized water and added directly into culture medium 12 h before treatment with 20 μM noscapine or 1 μM paclitaxel. The protein level and activity of JNK and the percentage of apoptotic cells were measured 48 h after drug treatment. JNK protein levels were measured by Western blot analysis performed on the immunoprecipitates and JNK activity was measured by the chemiluminescent Western blot analysis as described above. Morphological changes in the nuclear chromatin of cells were detected by staining with propidium iodide as a measure of apoptosis.

Transient Transfections—1A9, 1A9PTX10, and 1A9PTX22 cells grown on glass coverslips in 6-well plates were transfected either with 1 μg of pCDNA3(FLAG)-JNK-dn or with 1 μg of pCDNA3(FLAG) as a control, using FuGENE 6 reagent (Roche Molecular Biochemicals) according to the manufacturer's protocol. Cells were treated with 20 μM noscapine or 1 μM paclitaxel 12 h after transfection. The expression of JNK-dn, the activity of JNK, and the percentage of apoptotic cells were measured 48 h after drug treatment. To measure the expression of JNK-dn, cell lysates were immunoprecipitated with anti-JNK antibodies, and Western blot analysis was then performed on the immunoprecipitates, using a mouse monoclonal antibody against the FLAG tag to detect the FLAG-tagged JNK-dn. JNK activity was measured by the chemiluminescent Western blot analysis as described above. Transfected cells were identified with the anti-FLAG antibody, and morphological changes in the nuclear chromatin of transfected cells were detected by staining with propidium iodide as a measure of apoptosis.

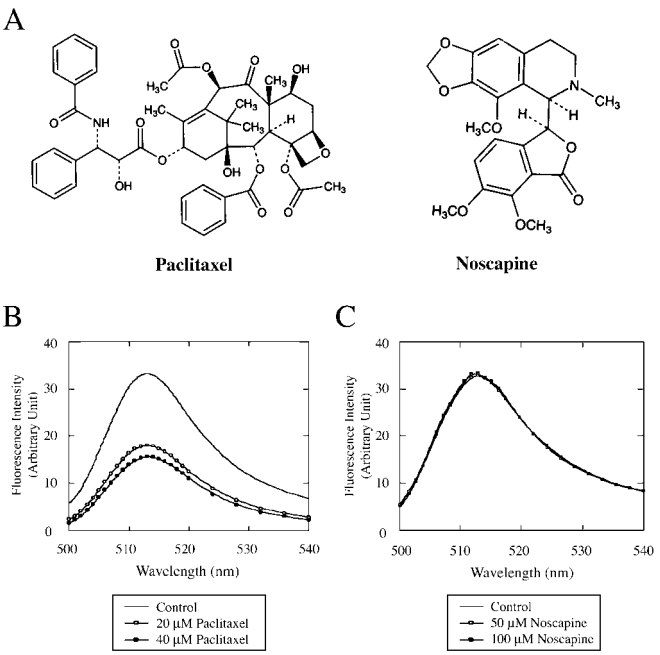

FIG. 1. **Noscapine does not inhibit paclitaxel binding to tubulin.** *A*, structures of noscapine and paclitaxel. In *B* and *C*, microtubules were polymerized from purified goat brain tubulin in the presence of 10% Me_2SO, and preformed microtubules were incubated with different concentrations of paclitaxel (20 and 40 μM), noscapine (50 and 100 μM), or the vehicle solution Me_2SO alone as a control. Fluorescent paclitaxel was then added to each of these solutions and the fluorescence intensity was measured at wavelengths ranging from 500 to 540 nm. The excitation wavelength was 490 nm. Unlabeled paclitaxel markedly inhibits the binding of fluorescent paclitaxel to tubulin, as evident from the reduction of the fluorescence intensity by unlabeled paclitaxel in a concentration-dependent manner (*B*). In contrast, 50 or even 100 μM noscapine does not inhibit the binding of fluorescent paclitaxel to tubulin, displaying intensity-wavelength curves overlapping with the control (*C*).

RESULTS

Noscapine Does Not Compete with Paclitaxel for Tubulin Binding—The binding conformation of paclitaxel in tubulin has recently been resolved (32–34). The binding pocket of paclitaxel resides in a deep hydrophobic cleft near the luminal surface of β-tubulin, where it interacts with the protein by means of three potential hydrogen bonds and multiple hydrophobic contacts (34). As an initial step to gain structural insights into the interactions between noscapine and tubulin, we asked whether noscapine binds to tubulin at sites common with paclitaxel. To test this, we performed a drug competition experiment using fluorescent paclitaxel (Fig. 1). We found that preincubation of microtubules assembled *in vitro* from purified $\alpha\beta$-tubulin with unlabeled paclitaxel significantly inhibited the binding of fluorescent paclitaxel to tubulin, as evident from the reduction of the fluorescence intensity by unlabeled paclitaxel in a concentration-dependent manner (Fig. 1*B*). In contrast, 50 or even 100 μM noscapine did not inhibit the binding of fluorescent paclitaxel to tubulin, displaying intensity-wavelength curves overlapping with the control (Fig. 1*C*). These results show that noscapine is unable to compete with paclitaxel for binding to tubulin, suggesting that noscapine binds to a site other than the paclitaxel-binding site.

Noscapine Inhibits the Proliferation of Both Paclitaxel-sensitive and Paclitaxel-resistant Human Ovarian Carcinoma Cells—The noninhibitory effect of noscapine on the tubulin binding activity of paclitaxel suggested that paclitaxel-resistant human cancer cells might be sensitive to noscapine. To test this, we first examined the effect of noscapine on the cell cycle

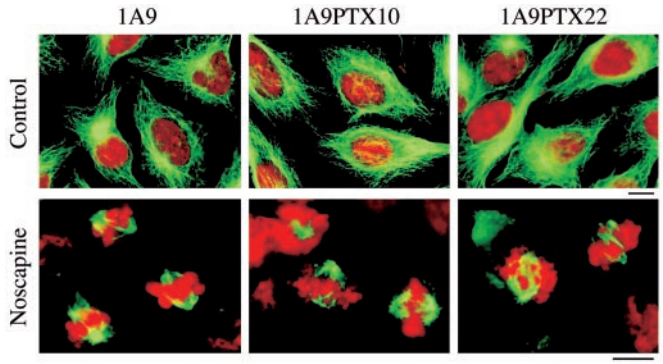

FIG. 2. **Immunofluorescence micrographs showing microtubules (*green*) and DNA (*red*) in human ovarian carcinoma cells treated with 20 μM noscapine for 18 h or the vehicle solution Me_2SO as a control.** The formation of nearly normal bipolar microtubule arrays (mitotic spindles) in noscapine-treated cells (*bottom panels*) indicates mitotic arrest (the mitotic indices in 1A9, 1A9PTX10, and 1A9PTX22 cells are 37.6, 35.2, and 35.8%, respectively). In contrast, only 5.4, 5.0, and 5.1% of the control 1A9, 1A9PTX10, and 1A9PTX22 cells were in mitosis, and the rest of them were in interphase (*upper panels*), showing typical radial microtubule arrays. *Bars*, 10 μm.

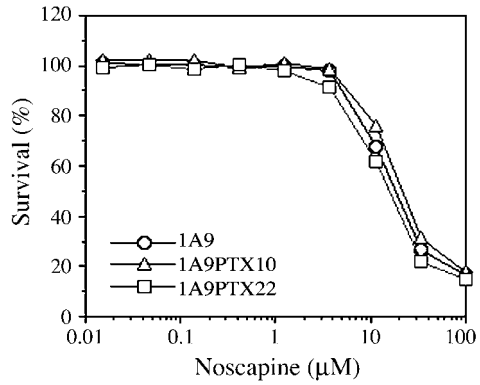

FIG. 3. **Noscapine causes cell death in paclitaxel-resistant, β-tubulin mutant 1A9PTX10 and 1A9PTX22 cell lines as effectively as for their parental cell line 1A9.** Cells were treated with noscapine for 72 h and the survival percentage was then measured by the sulforhodamine B assay as described under "Experimental Procedures." Each value represents the average of three independent experiments with duplicate determinations.

progression of a set of human ovarian carcinoma cells, including the parent cell line 1A9, which is sensitive to paclitaxel treatment, and two derivative paclitaxel-resistant lines, 1A9PTX10 and 1A9PTX22 (12). The two paclitaxel-resistant cell lines harbor β-tubulin mutations, F270V in 1A9PTX10 cells and A364T in 1A9PTX22 cells, that might interfere with paclitaxel binding to tubulin. In addition, 1A9PTX10 and 1A9PTX22 cells exhibit impaired paclitaxel-driven tubulin polymerization (12). We found that noscapine was able to arrest these human ovarian carcinoma cells at mitosis. For example, the mitotic indices for 1A9, 1A9PTX10, and 1A9PTX22 cells were 37.6, 35.2, and 35.8%, respectively, after treatment with 20 μM noscapine for 18 h. The noscapine-arrested cells have condensed chromosomes with nearly normal bipolar mitotic spindles (Fig. 2, *bottom panels*). In contrast, only 5.4, 5.0, and 5.1% of the control 1A9, 1A9PTX10, and 1A9PTX22 cells were in mitosis, and the rest of them were in interphase showing typical radial microtubule arrays (Fig. 2, *upper panels*).

We then used the sulforhodamine B assay to examine the effect of noscapine on the proliferation of these human ovarian carcinoma cells after a 72-h treatment (24). Our results revealed that noscapine inhibited the proliferation of 1A9, 1A9PTX10, and 1A9PTX22 cells with similar IC_{50} values (18.2, 22.7, and 15.4 μM, respectively) (Fig. 3). The inhibitory effects of noscapine on the proliferation of both paclitaxel-sensitive and paclitaxel-resistant cells are consistent with the notion that noscapine might bind to tubulin at a site different from that for paclitaxel, as indicated by the drug competition experiment (Fig. 1).

Noscapine Induces Apoptosis in Human Ovarian Carcinoma Cells—Because noscapine can induce apoptosis in a variety of tumor cell lines (13, 14), we asked whether the human ovarian carcinoma cell line 1A9 and its derivative paclitaxel-resistant cell lines underwent apoptotic cell death upon noscapine treatment. We first performed immunofluorescence microscopy to examine the apoptotic percentages, based on the nuclear morphology, of these cells upon treatment with 20 μM noscapine. As shown in Table I, the ratio of noscapine-treated cells with apoptotic morphology increased dramatically over time and reached more than 60% after 48 h of treatment. In addition, there was no obvious difference in the apoptotic cell ratio among 1A9, 1A9PTX10, and 1A9PTX22 cell lines.

To confirm that noscapine-treated human ovarian carcinoma cells died through the apoptosis pathway, we performed

TABLE I

Apoptotic percentages of human ovarian carcinoma cells after being treated with 20 μM noscapine for 0, 12, 24, 36, or 48 h

Values shown here are the averages and standard deviations of three independent experiments.

Assays of detection	Apoptotic cell ratio (%)		
	1A9	1A9PTX10	1A9PTX22
Nuclear morphology			
0 h	0.37 ± 0.09	0.41 ± 0.11	0.69 ± 0.17
12 h	7.39 ± 1.32	7.14 ± 1.21	7.45 ± 1.40
24 h	20.7 ± 4.1	21.3 ± 5.8	22.3 ± 5.1
36 h	37.4 ± 7.1	37.2 ± 9.7	39.1 ± 8.0
48 h	66.1 ± 12.8	63.8 ± 11.3	67.5 ± 11.7
TUNEL assay			
0 h	2.83 ± 0.32	3.39 ± 0.47	3.14 ± 0.38
12 h	7.44 ± 1.10	7.91 ± 1.25	7.09 ± 0.97
24 h	17.6 ± 2.5	16.7 ± 2.7	16.2 ± 2.1
36 h	39.5 ± 5.2	37.2 ± 4.3	39.1 ± 4.8
48 h	56.2 ± 7.8	50.2 ± 8.1[a]	60.8 ± 7.6[a]
Annexin V staining			
0 h	0.42 ± 0.12	0.38 ± 0.09	0.43 ± 0.10
12 h	11.2 ± 1.65	9.52 ± 1.47	8.18 ± 1.51
24 h	37.4 ± 5.4	34.1 ± 4.9	39.4 ± 5.5
36 h	53.1 ± 5.9	51.1 ± 6.1	57.2 ± 5.8[a]
48 h	60.8 ± 7.5	58.6 ± 8.0	66.9 ± 8.4[a]

[a] Results are significantly different when compared with the 1A9 group ($p < 0.05$).

TUNEL assay, which detects the fragmentation of DNA, a characteristic of cells undergoing apoptotic cell death (35). As shown in Fig. 4*A*, the apoptotic nuclei stained bright green because of the fluorescence of FITC and were easily identified in cells treated with 20 μM noscapine. The percentage of TUNEL-positive cells increased with the time of noscapine treatment, indicating the occurrence of apoptosis. After 48 h of treatment, as many as 56.2, 50.2, and 60.8% of 1A9, 1A9PTX10, and 1A9PTX22 cells, respectively, displayed TUNEL-positive staining (Table I).

We then took another approach to quantify apoptotic cell ratio, annexin V-FITC staining assay, which reports the loss of phosphatidylserine asymmetry of plasma membrane at the early stage of apoptosis (36). Fig. 4*B* shows representative annexin V-FITC staining profiles at two time points after noscapine treatment, 0 and 24 h, respectively. Similar to that measured by the TUNEL assay, the percentage of annexin V-FITC-positive cells increased over time and reached 60.8, 58.6, and 66.9%, for 1A9, 1A9PTX10, and 1A9PTX22 cells, respectively, after 48 h of noscapine treatment (Table I).

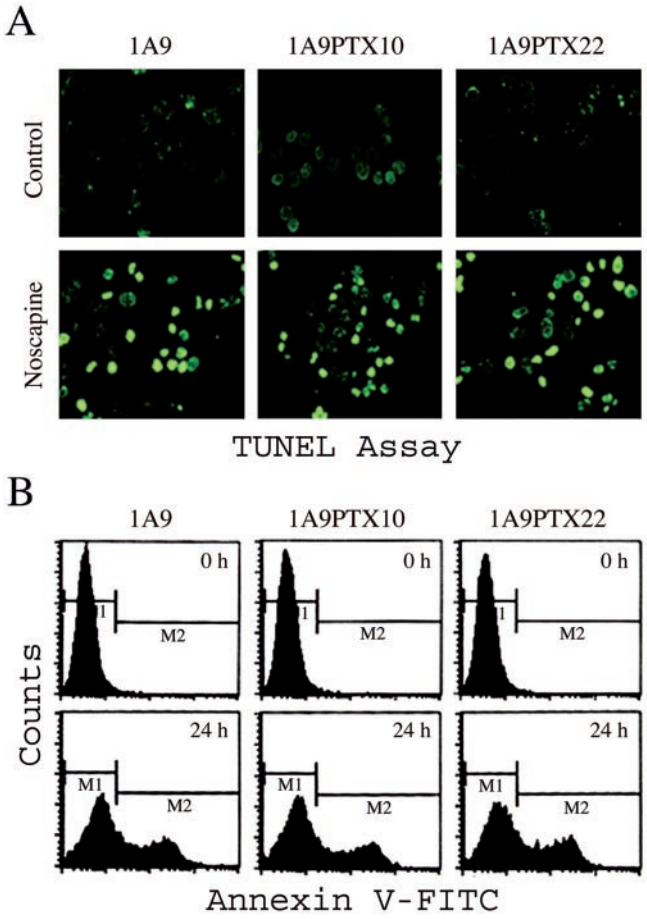

FIG. 4. **Noscapine induces apoptosis in human ovarian carcinoma cells as revealed by TUNEL assay (*A*) and annexin V-FITC staining assay (*B*).** *A*, a group of representative TUNEL assay results, showing that TUNEL-positive cells stained *bright green*. *B*, representative annexin V-FITC staining profiles of cells treated with noscapine for 0 h (*upper panels*) and 24 h (*bottom panels*). The *M1* and *M2* gates demarcate annexin V-FITC negative and positive staining populations, respectively. Please see Table I for a summary of the quantitation of TUNEL and annexin V-FITC positive 1A9, 1A9PTX10, and 1A9PTX22 cells after 0, 12, 24, 36, or 48 h of noscapine treatment.

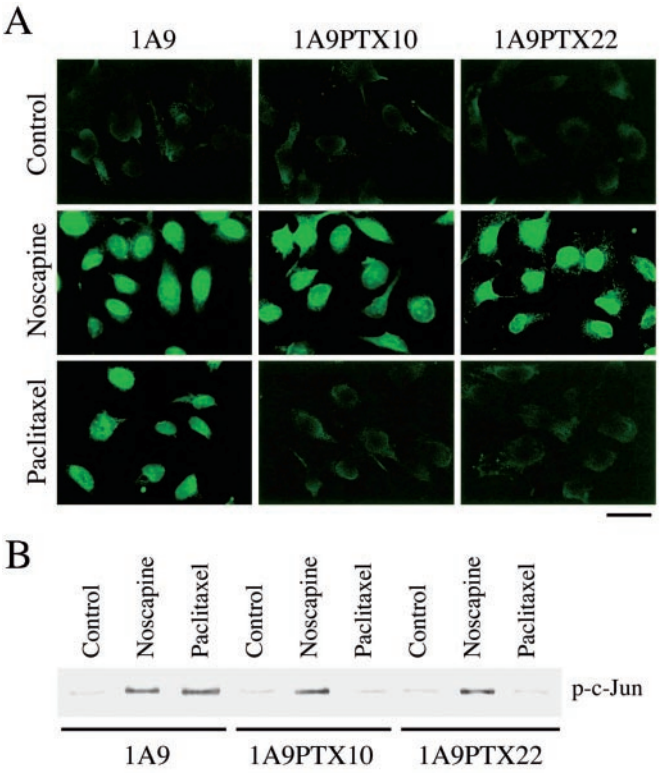

FIG. 5. **Phosphorylation of c-Jun in human ovarian carcinoma cells treated with noscapine.** *A*, immunofluorescence micrographs showing the extent of c-Jun phosphorylation in 1A9, 1A9PTX10, and 1A9PTX22 cells treated with 20 μM noscapine, 1 μM paclitaxel, or the vehicle solution Me_2SO for 12 h. Phosphorylation of c-Jun was visualized using antibodies against phosphorylated c-Jun as described under "Experimental Procedures." *Bar*, 10 μm. *B*, Western blot analysis for the level of phosphorylated c-Jun (p-c-Jun) in the nuclei of 1A9, 1A9PTX10, and 1A9PTX22 cells upon treatment with Me_2SO, 20 μM noscapine, or 1 μM paclitaxel for 12 h. Nuclear extracts were prepared by the method of Stone and Chambers (28), and Western blotting was performed using antibodies against phosphorylated c-Jun.

The results achieved from the above three different apoptosis detection assays were strikingly comparable with each other. These assays showed similar apoptotic cell ratios for each individual cell line upon noscapine treatment. In addition, they all revealed a time-dependent increase in the percentage of apoptotic cells after being treated with noscapine.

JNK Activation upon Noscapine Treatment—The JNK, also known as stress-activated protein kinases, are a group of mitogen-activated protein kinases that bind the NH_2-terminal activation domain of the transcription factor c-Jun and phosphorylate c-Jun on amino acid residues Ser-63 and Ser-73 (37–39). JNK has been implicated in the regulation of cell proliferation, tumor transformation, and apoptosis as well as embryonic morphogenesis (40). JNK is activated when cells are exposed to proinflammatory cytokines or environmental stress (*e.g.* UV- and γ-radiation, heat shock, osmotic shock, redox stress, etc.), or undergo growth factor withdrawal (40). Recently, JNK activation has also been found in cells treated with antimicrotubule agents (28, 29, 41–43). Furthermore, the JNK pathway has been demonstrated to be required for apoptosis caused by these agents (41, 43). It is thus conceivable that the JNK pathway might also play a role in noscapine-induced apoptosis in 1A9, 1A9PTX10, and 1A9PTX22 cells.

To test this, we first examined the activity of JNK in noscapine-treated human ovarian carcinoma cells by measuring the level of endogenous phosphorylated c-Jun. As revealed by Fig. 5*A*, 12 h after noscapine treatment, the level of endogenous phosphorylated c-Jun was markedly increased in these cells showing bright fluorescence signal in the nuclei, indicating JNK activation because of noscapine treatment. In contrast, 1 μM paclitaxel could activate JNK in 1A9 cells but not in the two mutant cell lines that are resistant to paclitaxel (Fig. 5*A*). We used 1 μM rather than 20 μM paclitaxel as a control for noscapine experiments in this study (also see figures below), because of the devastating cytotoxicity of paclitaxel at high concentrations.

We then performed a Western blot analysis of nuclear extracts to further examine the level of endogenous phosphorylated c-Jun in 1A9, 1A9PTX10, and 1A9PTX22 cells in response to noscapine treatment (Fig. 5*B*). Nuclear extracts were prepared using the method of Stone and Chambers (28) and then subjected to Western blotting with antibodies against phosphorylated c-Jun. Consistent with the immunofluorescence staining results (Fig. 5*A*), the phosphorylation of c-Jun could be clearly visualized as early as 12 h of noscapine treatment in all three human ovarian carcinoma cell lines; however, upon paclitaxel treatment, c-Jun was phosphorylated only in the 1A9 cell line (Fig. 5*B*). We also performed immunofluorescence staining and Western blotting with a phosphorylation independent c-Jun antibody and found that the level of endogenous c-Jun remained constant in 1A9, 1A9PTX10, and 1A9PTX22

cells following treatment with noscapine or paclitaxel.[2]

To further investigate JNK activation in response to noscapine treatment, we examined JNK activity by immunocomplex JNK activity assay (through the chemiluminescent Western blot analysis with antibodies against phosphorylated c-Jun) in 1A9, 1A9PTX10, and 1A9PTX22 cells after they were treated with 20 μM noscapine for 0, 12, 24, 36, or 48 h. As shown in Fig. 6*A*, noscapine induced the activation of JNK in a time-dependent manner in all three cell lines. In contrast, paclitaxel induced JNK activation only in the parental cell line 1A9. We quantified the level of JNK activation by measuring the level of phosphorylated c-Jun with densitometry and compared the effect of noscapine with paclitaxel (Table II). After 12, 24, 36, and 48 h of noscapine treatment, the JNK activity in 1A9 cells was 3.3-, 4.5-, 4.8-, and 6.9-fold, respectively, as high as that for the untreated 1A9 cells. In contrast, the -fold of JNK activation was 2.9, 4.4, 4.9, and 7.1, respectively, for 1A9PTX10 cells, and 3.1, 3.9, 4.2, and 6.6, respectively, for 1A9PTX22 cells, in response to 12, 24, 36, and 48 h of noscapine treatment (Table II). In 1A9 cells treated with 1 μM paclitaxel for 12, 24, 36, and 48 h, the JNK activity was 3.6-, 4.7-, 5.3-, and 7.9-fold, respectively, as high as that for the untreated 1A9 cells (Table II). However, in 1A9PTX10 and 1A9PTX22 cells treated with 1 μM paclitaxel, the activity of JNK was similar to that of the untreated, indicating that JNK was not activated by paclitaxel in these mutant cell lines.

To confirm that the JNK activity assay is quantitative, we examined the linearity of this assay (Fig. 6*B*). Strikingly, phosphorylation of c-Jun occurred linearly (the arbitrary densitometry units were 0.91, 1.43, 2.29, 3.64, 5.68, and 9.25, respectively) over a 16.67-fold range of the JNK enzyme (ranging from 30 to 500 microunits), under the same condition as that for the immunocomplex JNK activity assay except that pure active JNK instead of the JNK immunoprecipitate was used (Fig. 6*B*, *left panel*). Furthermore, phosphorylation of c-Jun also occurred linearly over 40 min of incubation time (Fig. 6*B*, *right panel*).

We also examined the specificity of the immunoprecipitation procedure. Protein A-agarose beads alone and protein A-agarose beads plus antibodies against hemagglutinin, an unrelated antibody, were used as controls (Fig. 6*C*). We found that JNK protein was immunoprecipitated and showed activity only when both protein A-agarose beads and JNK antibody were used (Fig. 6*C*). We thus conclude that JNK is indeed activated to a significant extent in response to noscapine treatment.

The JNK Pathway Is Required for Noscapine-induced Apoptosis—To test whether the observed JNK activation plays a role in noscapine-induced apoptosis, we selectively inhibited JNK activity by using JNK-specific antisense oligonucleotides that have proven highly effective in the inhibition of JNK expression in human cells (30, 31). 1A9, 1A9PTX10, and 1A9PTX22 cells were incubated with the antisense oligonucleotides for 12 h before treatment with noscapine. Consequently, the protein level of JNK in these human ovarian carcinoma cells was significantly reduced, and noscapine-induced JNK activation was also remarkably blocked (Fig. 7). In contrast, cells incubated with the solvent alone or with sense oligonucleotides exhibited much higher JNK protein levels and activity. We then examined the percentage of apoptotic cells under these conditions. JNK antisense oligonucleotides clearly prevented 1A9, 1A9PTX10, and 1A9PTX22 cells from undergoing apoptosis, however, the solvent alone or sense oligonucleotides did not (Fig. 7). One μM paclitaxel was also used as a control to examine the effect of oligonucleotide treatment on JNK protein level and activity and the apoptotic percentage. Strikingly, 1A9 cells, but not 1A9PTX10 and 1A9PTX22 cells, were sensitive to

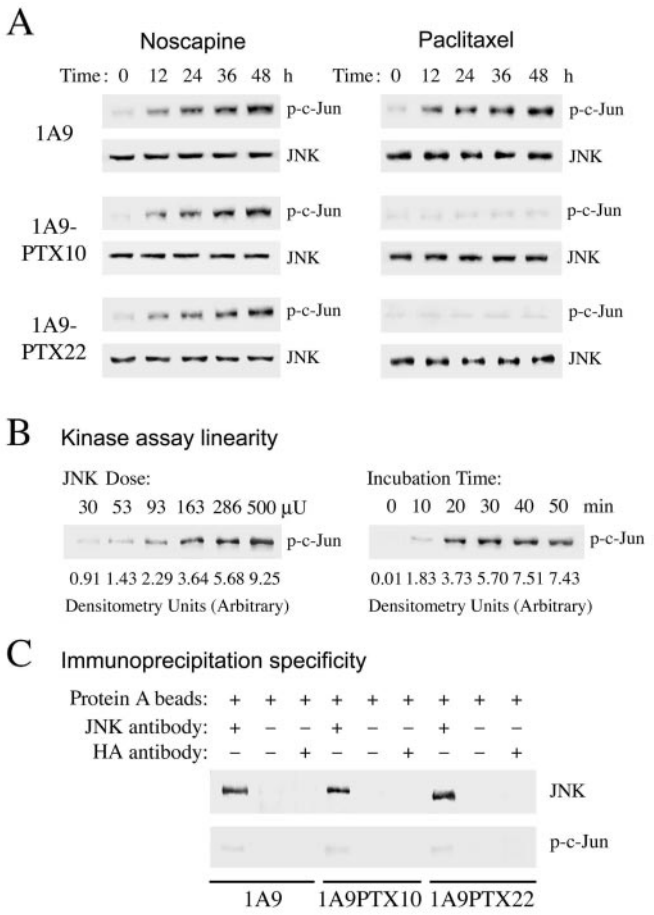

FIG. 6. **JNK activation upon noscapine treatment.** *A*, measurement of JNK activity in 1A9, 1A9PTX10, and 1A9PTX22 cells after treatment with 20 μM noscapine or 1 μM paclitaxel for 0, 12, 24, 36, or 48 h (*upper panels*). JNK activity was measured by chemiluminescent Western blot analysis using antibodies against phosphorylated c-Jun (*p-c-Jun*) and described in detail under "Experimental Procedures." The level of p-c-Jun was determined by densitometry (arbitrary units). Each experiment was repeated three times with duplicate densitometric determinations (see Table II for a summary of the quantitation of JNK activity in noscapine- and paclitaxel-treated 1A9, 1A9PTX10, and 1A9PTX22 cells). To confirm that equal amounts of JNK were used for kinase reactions, the level of JNK protein was measured by Western blot analysis (performed on the immunoprecipitates derived from cell extracts containing 100 μg of total protein) (*bottom panels*). *B*, linearity of the JNK activity assay. The level of p-c-Jun was determined by densitometry (arbitrary units) as a measure of JNK activity, and each value represents the average of three independent experiments with duplicate determinations. *Left panel*, phosphorylation of c-Jun occurs linearly over a 16.67-fold range of the JNK enzyme under the same conditions as that for *A* except that pure active JNK (ranging from 30 to 500 microunits) instead of JNK immunoprecipitate was used. 1 Unit of JNK is equal to 1 nM phosphate incorporated into glutathione *S*-transferase-c-Jun per min. *Right panel*, phosphorylation of c-Jun occurs linearly over 40 min of incubation time and then attenuates. The kinase reaction was performed under the same conditions as that for *A* except that pure active JNK (286 microunits) instead of JNK immunoprecipitate was used, and the incubation time ranged from 0 to 50 min instead of a constant time of 30 min. *C*, specificity controls for immunoprecipitation. Protein A-agarose beads alone and protein A-agarose beads plus antibodies against hemagglutinin, an unrelated antibody, were used as controls. Preparation of whole cell lysates of untreated 1A9, 1A9PTX10, and 1A9PTX22 cells, immunoprecipitation, kinase assay, and Western blot analysis were performed as in *A*. Note that JNK protein was immunoprecipitated (*upper panel*) and showed activity (*bottom panel*) only when both protein A-agarose beads and JNK antibody were used, confirming the specificity of the immunoprecipitation procedure.

[2] J. Zhou, K. Gupta, J. Yao, K. Ye, D. Panda, P. Giannakakou, and H. C. Joshi, unpublished data.

TABLE II
JNK activity in noscapine- and paclitaxel-treated human ovarian carcinoma cells

JNK activity was determined by measuring the level of phosphorylated c-Jun with densitometry as described in the legend to Fig. 6*A* and under "Experimental Procedures." Relative JNK activity refers to the values relative to those in untreated groups (0 h). Values shown in this table are the averages and standard deviations of three independent experiments with duplicate determinations.

Treatment	Relative JNK activity		
	1A9	1A9PTX10	1A9PTX22
Noscapine (20 μM)			
0 h	1.0	1.0	1.0
12 h	3.3 ± 0.7	2.9 ± 0.4	3.1 ± 0.8
24 h	4.5 ± 0.6	4.4 ± 0.7	3.9 ± 1.0
36 h	4.8 ± 1.1	4.9 ± 1.3	4.2 ± 0.7
48 h	6.9 ± 1.2	7.1 ± 1.5	6.6 ± 1.1
Paclitaxel (1 μM)			
0 h	1.0	1.0	1.0
12 h	3.6 ± 0.8	0.9 ± 0.02	0.8 ± 0.04
24 h	4.7 ± 0.9	1.1 ± 0.03	1.2 ± 0.03
36 h	5.3 ± 1.2	1.2 ± 0.03	0.9 ± 0.02
48 h	7.9 ± 1.4	1.0 ± 0.02	1.0 ± 0.03

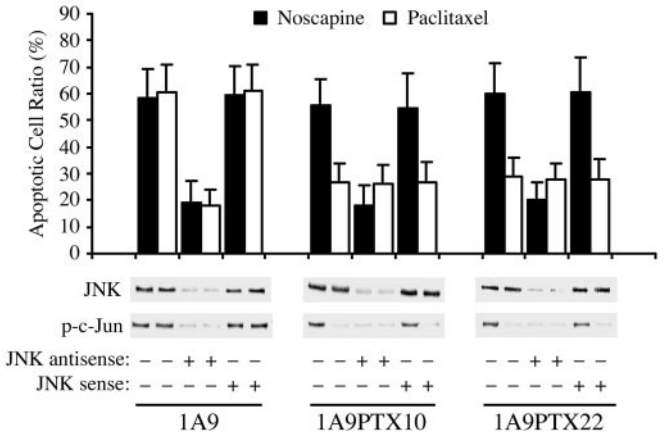

FIG. 7. **Inhibition of JNK activity by specific antisense oligonucleotide blocks noscapine-induced apoptosis in human ovarian cancer cells.** The oligonucleotides were synthesized in phosphorothioate-modified conditions and purified by high performance liquid chromatography and added directly into culture medium 12 h before treatment with 20 μM noscapine or 1 μM paclitaxel. JNK-specific sense oligonucleotide and the solvent, sterilized water, were used as controls for the JNK-specific antisense oligonucleotide. The protein level and activity of JNK and the percentage of apoptotic cells were measured 48 h after treatment with noscapine or paclitaxel. JNK protein levels were measured by Western blot analysis performed on the immunoprecipitates and JNK activity was measured by chemiluminescent Western blot analysis as described in the legend to Fig. 6*A* and under "Experimental Procedures." Note that JNK protein levels in 1A9, 1A9PTX10, and 1A9PTX22 cells have significantly decreased upon antisense oligonucleotide treatment. Morphological changes in the nuclear chromatin of cells were detected by staining with propidium iodide as a measure of apoptosis. Values and *error bars* shown in this graph represent the averages and standard deviations, respectively, of three independent experiments. *p-c-Jun* stands for phosphorylated c-Jun.

paclitaxel-induced JNK activation and apoptosis, which were inhibited by treatment with the JNK antisense oligonucleotides (Fig. 7). These results thus indicate that the JNK pathway is required for human ovarian carcinoma cells to undergo apoptosis upon noscapine treatment.

We tested this idea further by inhibition of JNK activity through dominant negative transfections. 1A9, 1A9PTX10, and 1A9PTX22 cells were transiently transfected with pCDNA3(FLAG)-JNK-dn, which expresses a dominant allele of JNK with a FLAG tag (44), and then treated these cells with 20 μM noscapine or 1 μM paclitaxel as a control. As shown in Fig.

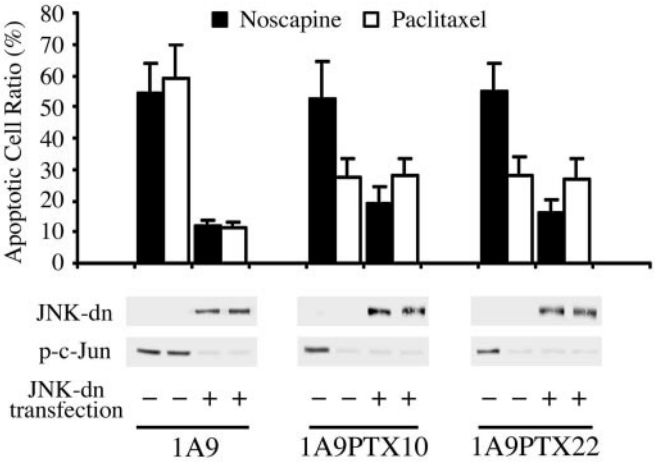

FIG. 8. **Inhibition of JNK activity by transient transfection of dominant negative JNK (*JNK-dn*) prevents noscapine-induced apoptosis in human ovarian cancer cells.** 1A9, 1A9PTX10, and 1A9PTX22 cells grown on glass coverslips in 6-well plates were transfected either with 1 μg of pCDNA3(FLAG)-JNK-dn or with 1 μg of pCDNA3(FLAG) as a control, as described under "Experimental Procedures." Cells were treated with 20 μM noscapine or 1 μM paclitaxel 12 h after transfection. The expression of JNK-dn, the activity of JNK, and the percentage of apoptotic cells were measured 48 h after drug treatment. To measure the expression of JNK-dn, cell lysates were immunoprecipitated with anti-JNK antibodies, and Western blot analysis was then performed on the immunoprecipitates using a mouse monoclonal antibody against the FLAG tag to detect the FLAG-tagged JNK-dn. JNK activity was measured by the chemiluminescent Western blot analysis as in Fig. 6*A* and described under "Experimental Procedures." Transfected cells were identified with the anti-FLAG antibody, and morphological changes in the nuclear chromatin of transfected cells were detected by staining with propidium iodide as a measure of apoptosis. Values and *error bars* shown in this graph represent the averages and standard deviations, respectively, of three independent experiments. *p-c-Jun* stands for phosphorylated c-Jun.

8, JNK activity was largely blocked by expression of the dominant negative allele. For 1A9, 1A9PTX10, and 1A9PTX22 cells expressing the dominant negative JNK, only 11.9, 21.2, and 18.9% of the cells underwent apoptosis, respectively, after 48 h of noscapine treatment. In contrast, for cells transfected with the control plasmid, as many as 53.2, 51.0, and 54.9% of the cells underwent apoptosis, respectively, upon noscapine treatment (Fig. 8). In addition, 1A9 cells, but not 1A9PTX10 and 1A9PTX22 cells, were sensitive to paclitaxel-induced JNK activation and apoptosis, which were inhibited by expression of the dominant negative JNK (Fig. 8). Thus, we conclude that the JNK pathway is required for noscapine-induced apoptosis in human ovarian carcinoma cells.

DISCUSSION

Microtubules are highly dynamic polymers that are crucial for accurate chromosome segregation during mitosis through formation of the bipolar mitotic spindle. To ensure faithful chromosome transmission, eukaryotic cells have evolved a surveillance mechanism called the spindle assembly checkpoint, which halts mitotic progression when the spindle has a defect or chromosomes are not properly attached by spindle microtubules (45). It is not surprising then that many chemical compounds that target microtubules can arrest cells at mitosis, a property attributed to the use of microtubule targeting agents in cancer chemotherapy. Notable examples are paclitaxel, docetaxel, and the vinca alkaloids, which have proven successful in clinical use (5–8). However, the clinical applicability of these microtubule targeting drugs is hampered by their low aqueous solubility and toxicity. Moreover, although patients have impressive initial response to these drugs, many of them relapse after treatment because of the development of drug resistance.

Consequently, considerable effort has been made over the past decade to develop and/or discover novel antimicrotubule agents that have similar modes of action to the currently used drugs but with improved biological and pharmaceutical features.

During a systematic screen based on structural similarity of known microtubule targeting agents, we have identified the opium alkaloid noscapine as a microtubule targeting agent (13). Noscapine acts mechanistically similar to many other microtubule agents, in that it binds to the tubulin subunit of microtubules, alters microtubule dynamics, blocks mitotic progression, causes apoptosis, and has potent antitumor activity (13–15). In this study, we demonstrate that noscapine can effectively inhibit the proliferation and induce apoptosis in both paclitaxel-sensitive and paclitaxel-resistant (because of β-tubulin mutations that affect paclitaxel binding) human ovarian carcinoma cells. This is in agreement with the assumption that noscapine binds to tubulin at a site different from the paclitaxel-binding site, as indicated by the noninhibitory effect of noscapine on paclitaxel binding to tubulin (Fig. 1). It will be of great importance to test in the nude mice model whether noscapine can inhibit the growth of tumors formed from the transplantation of paclitaxel-resistant human cancer cells.

Unlike many other microtubule targeting drugs, noscapine does not significantly promote or inhibit microtubule polymerization even at high concentrations, nor does it affect the total polymer mass of tubulin (15). When applied to tissue culture cells, noscapine does not cause gross deformations of cellular microtubules. Instead, noscapine alters the steady-state dynamics of microtubule assembly, which is sufficient to arrest mitosis (15). This unique feature of noscapine would assume that other microtubule-dependent cellular events such as organelle distribution and axonal transport are not affected, which are serious concerns for many currently used microtubule-targeting anticancer drugs. Indeed, noscapine has been found to cause little or no toxicity to the kidney, heart, liver, bone marrow, spleen, or small intestine, and does not inhibit primary humoral immune responses in mice (19). Because noscapine is water-soluble and absorbed after oral administration (16–18), its chemotherapeutic potential in the treatment of human cancers merits thorough evaluation, particularly for cancers that are resistant to the currently used drugs.

Several lines of compelling evidence suggest that antimicrotubule agents are able to induce both morphological and biochemical features of the typical apoptosis, including chromatin condensation, cell membrane blebbing, and internucleosomal DNA fragmentation (46–52). It has been thought that this might result from the inhibition of microtubule polymerization or depolymerization. Because noscapine suppresses microtubule dynamics without obvious effects on microtubule polymerization or depolymerization (15), yet can induce characteristic apoptosis in a variety of cell types (Fig. 4; also see Refs. 13 and 14), we propose that apoptotic cell death caused by antimicrotubule agents might reflect the disruption of the normal physiological balance in microtubule dynamics rather than the action of them on the polymerization and depolymerization of microtubules.

It has been suggested that antimicrotubule agents might trigger apoptosis through a variety of phosphoregulatory pathways. For example, signal transduction pathways mediated by Ras, Raf-1, and ASK1 (apoptosis signal-regulating kinase) have been implicated in apoptosis induced by paclitaxel (29, 41). The JNK pathway, which was initially thought to participate in apoptosis induced by environmental stress, proinflammatory cytokines, or growth factor withdrawal (40), has been recently shown to play a role in microtubule dysfunction-induced apoptosis as well (41, 43). It is thus understandable that noscapine, being a microtubule targeting agent, induces apoptosis through a similar mechanism.

JNK activation has been observed in cells treated with microtubule targeting agents such as paclitaxel and vinblastine (28, 29, 41–43). In addition, activation of JNK by paclitaxel has been suggested to require interactions between microtubules and paclitaxel (29). We find that noscapine causes nearly equal JNK activation among human ovarian carcinoma cell lines 1A9 and the two derivative, β-tubulin mutant cell lines, 1A9PTX10 and 1A9PTX22 (Figs. 5 and 6). This finding is consistent with the observation that paclitaxel caused JNK activation only in the parental 1A9 line but not in the two derivative lines harboring β-tubulin mutations that impair paclitaxel binding to tubulin (Figs. 5–8). Our data suggest that these mutations do not affect noscapine interactions with tubulin nor the downstream effects leading to apoptosis. In addition, our data also support the notion that noscapine does not bind at the paclitaxel site on tubulin. At present, it remains unclear how the microtubule interactions of microtubule targeting agents mediates the activation of JNK, which in turn leads to the occurrence of apoptosis. The level of JNK activity in the untreated ovarian carcinoma cells may appear slightly high relative to some other reports in the field (see for example, Ref. 41). Therefore, it is possible that the JNK pathway may be already slightly activated in these cells before the experiments start because of their being cultured in paclitaxel-containing medium 7 days prior to the experiments.

Taken together, we describe here that the antimicrotubule agent noscapine is highly effective in inhibiting proliferation and inducing apoptosis in human ovarian carcinoma cells sensitive or resistant to paclitaxel. In addition, we demonstrate that the JNK pathway plays a role in noscapine-induced apoptosis. In the future, it will be of great interest to explore the use of noscapine in the treatment of paclitaxel-resistant human cancers. A better understanding of the molecular mechanisms by which JNK mediates the apoptotic cell death induced by noscapine may also facilitate its use in cancer chemotherapy.

Acknowledgments—We thank Dr. Roger J. Davis for reagents and Drs. Erica Werner, Victor Faundez, Timothy C. Chambers, Haian Fu, John C. Lucchesi, Guy M. Benian, Dennis C. Liotta, James P. Snyder, and James H. Nettles for helpful discussions and many good suggestions. We are greatly indebted to the anonymous reviewers for extremely helpful suggestions about experiments.

REFERENCES

1. McIntosh, J. R. (1994) in *Microtubules* (Hyams, J. S., and Lloyd, C. W., eds) pp. 413–434, Wiley-Liss, Inc., New York
2. Mitchison, T., and Kirschner, M. (1984) *Nature* **312,** 237–242
3. Desai, A., and Mitchison, T. J. (1997) *Annu. Rev. Cell Dev. Biol.* **13,** 83–117
4. Jordan, M. A., and Wilson, L. (1999) *Methods Cell Biol.* **61,** 267–295
5. Rowinsky, E. K. (1997) *Annu. Rev. Med.* **48,** 353–374
6. Crown, J., and O'Leary, M. (2000) *Lancet* **355,** 1176–1178
7. van Tellingen, O., Sips, J. H., Beijnen, J. H., Bult, A., and Nooijen, W. J. (1992) *Anticancer Res.* **12,** 1699–1715
8. Haskell, C. M. (1995) in *Cancer Treatment* (Haskell, C. M., ed) pp. 78–165, W. B. Saunders Co., Philadelphia, PA
9. Gottesman, M. M., and Pastan, I. (1993) *Annu. Rev. Biochem.* **62,** 385–427
10. Bradley, G., and Ling, V. (1994) *Cancer Metastasis Rev.* **13,** 223–233
11. Burkhart, C. A., Kavallaris, M., and Horwitz, S. B. (2001) *Biochim. Biophys. Acta* **1471,** O1–O9
12. Giannakakou, P., Sackett, D. L., Kang, Y. K., Zhan, Z., Buters, J. T., Fojo, T., and Poruchynsky, M. S. (1997) *J. Biol. Chem.* **272,** 17118–17125
13. Ye, K., Ke, Y., Keshava, N., Shanks, J., Kapp, J. A., Tekmal, R. R., Petros, J., and Joshi, H. C. (1998) *Proc. Natl. Acad. Sci. U. S. A.* **95,** 1601–1606
14. Ye, K., Zhou, J., Landen, J. W., Bradbury, E. M., and Joshi, H. C. (2001) *J. Biol. Chem.* **276,** 46697–46700
15. Zhou, J., Panda, D., Landen, J. W., Wilson, L., and Joshi, H. C. (2002) *J. Biol. Chem.* **277,** 17200–17208
16. Dahlstrom, B., Mellstrand, T., Lofdahl, C. G., and Johansson, M. (1982) *Eur. J. Clin. Pharmacol.* **22,** 535–539
17. Haikala, V., Sothmann, A., and Marvola, M. (1986) *Eur. J. Clin. Pharmacol.* **31,** 367–369
18. Karlsson, M. O., Dahlstrom, B., Eckernas, S. A., Johansson, M., and Alm, A. T. (1990) *Eur. J. Clin. Pharmacol.* **39,** 275–279
19. Ke, Y., Ye, K., Grossniklaus, H. E., Archer, D. R., Joshi, H. C., and Kapp, J. A. (2000) *Cancer Immunol. Immunother.* **49,** 217–225

20. Hamel, E., and Lin, C. M. (1981) *Arch. Biochem. Biophys.* **209,** 29–40
21. Panda, D., Chakrabarti, G., Hudson, J., Pigg, K., Miller, H. P., Wilson, L., and Himes, R. H. (2000) *Biochemistry* **39,** 5075–5081
22. Bradford, M. M. (1976) *Anal. Biochem.* **72,** 248–254
23. Eva, A., Robbins, K. C., Andersen, P. R., Srinivasan, A., Tronick, S. R., Reddy, E. P., Ellmore, N. W., Galen, A. T., Lautenberger, J. A., Papas, T. S., Westin, E. H., Wong-Staal, F., Gallo, R. C., and Aaronson, S. A. (1982) *Nature* **295,** 116–119
24. Skehan, P., Stroreng, R., Scudiero, D., Monks, A., McMahon, J., Vistica, D., Warren, J. T., Bokesch, H., Kenney, S., and Boyd, M. R. (1990) *J. Natl. Cancer Inst.* **82,** 1107–1112
25. Zhou, J., Shu, H. B., and Joshi, H. C. (2002) *J. Cell. Biochem.* **84,** 472–483
26. Joshi, H. C., and Zhou, J. (2001) *Methods Cell Biol.* **67,** 179–193
27. Figueroa-Masot, X. A., Hetman, M., Higgins, M. J., Kokot, N., and Xia, Z. (2001) *J. Neurosci.* **21,** 4657–4667
28. Stone, A. A., and Chambers, T. C. (2000) *Exp. Cell Res.* **254,** 110–119
29. Wang, T. H., Wang, H. S., Ichijo, H., Giannakakou, P., Foster, J. S., Fojo, T., and Wimalasena, J. (1998) *J. Biol. Chem.* **273,** 4928–4936
30. Seimiya, H., Mashima, T., Toho, M., and Tsuruo, T. (1997) *J. Biol. Chem.* **272,** 4631–4636
31. Shiah, S. G., Chuang, S. E., Chau, Y. P., Shen, S. C., and Kuo, M. L. (1999) *Cancer Res.* **59,** 391–398
32. Nogales, E., Wolf, S. G., and Downing, K. (1998) *Nature* **391,** 121–123
33. Nogales, E., Whittaker, M., Milligan, R. A., and Downing, K. H. (1999) *Cell* **96,** 79–88
34. Snyder, J. P., Nettles, J. H., Cornett, B., Downing, K. H., and Nogales, E. (2001) *Proc. Natl. Acad. Sci. U. S. A.* **98,** 5312–5316
35. Heatwole, V. M. (1999) *Methods Mol. Biol.* **115,** 141–148
36. van Engeland, M., Nieland, L. J., Ramaekers, F. C., Schutte, B., and Reutelingsperger, C. P. (1998) *Cytometry* **31,** 1–9
37. Pulverer, B. J., Kyriakis, J. M., Avruch, J., Nikolakaki, E., and Woodgett, J. R. (1991) *Nature* **353,** 670–674
38. Adler, V., Polotskaya, A., Wagner, F., and Kraft, A. S. (1992) *J. Biol. Chem.* **267,** 17001–17005
39. Hibi, M., Lin, A., Smeal, T., Minden, A., and Karin, M. (1993) *Genes Dev.* **7,** 2135–2148
40. Davis, R. J. (2000) *Cell* **103,** 239–252
41. Wang, T. H., Popp, D. M., Wang, H. S., Saitoh, M., Mural, J. G., Henley, D. C., Ichijo, H., and Wimalasena, J. (1999) *J. Biol. Chem.* **274,** 8208–8216
42. Shtil, A. A., Mandlekar, S., Yu, R., Walter, R. J., Hagen, K., Tan, T. H., Roninson, I. B., and Kong, A. N. (1999) *Oncogene* **18,** 377–384
43. Fan, M., Goodwin, M. E., Birrer, M. J., and Chambers, T. C. (2001) *Cancer Res.* **61,** 4450–4458
44. Johnson, N. L., Gardner, A. M., Diener, K. M., Lange-Carter, C. A., Gleavy, J., Jarpe, M. B., Minden, A., Karin, M., Zon, L. I., and Johnson, G. L. (1996) *J. Biol. Chem.* **271,** 3229–3237
45. Zhou, J., Yao, J., and Joshi, H. C. (2002) *J. Cell Sci.* **115,** 3547–3555
46. Bhalla, K., Ibrado, A. M., Tourkina, E., Tang, C., Mahoney, M. E., and Huang, Y. (1993) *Leukemia* **7,** 563–568
47. Jordan, M. A., Toso, R. J., Thrower, D., and Wilson, L. (1993) *Proc. Natl. Acad. Sci. U. S. A.* **90,** 9552–9556
48. Jordan, M. A., Wendell, K., Gardiner, S., Derry, W. B., Copp, H., and Wilson, L. (1996) *Cancer Res.* **56,** 816–825
49. Bonfoco, E., Ceccatelli, S., Manzo, L., and Nicotera, P. (1995) *Exp. Cell Res.* **218,** 189–200
50. Woods, C. M., Zhu, J., McQueney, P. A., Bollag, D., and Lazarides, E. (1995) *Mol. Med.* **1,** 506–526
51. Kawamura, K. I., Grabowski, D., Weizer, K., Bukowski, R., and Ganapathi, R. (1996) *Br. J. Cancer* **73,** 183–188
52. Yu, D., Jing, T., Liu, B., Yao, J., Tan, M., McDonnell, T. J., and Hung, M. C. (1998) *Mol. Cell* **2,** 581–591